

Dry etching of TaN / HfO₂ gate-stack structure in BCl₃ / Ar / O₂ inductively coupled plasmas

Cite as: J. Vac. Sci. Technol. A **24**, 1373 (2006); <https://doi.org/10.1116/1.2210944>
Submitted: 05 May 2005 • Accepted: 15 May 2006 • Published Online: 22 June 2006

M. H. Shin, M. S. Park, N.-E. Lee, et al.



View Online



Export Citation

ARTICLES YOU MAY BE INTERESTED IN

[Dry etching characteristics of TiN film using Ar/CHF₃, Ar/Cl₂, and Ar/BCl₃ gas chemistries in an inductively coupled plasma](#)


Journal of Vacuum Science & Technology B: Microelectronics and Nanometer Structures Processing, Measurement, and Phenomena **21**, 2163 (2003); <https://doi.org/10.1116/1.1612517>

[Etching mechanisms of HfO₂, SiO₂, and poly-Si substrates in BCl₃ plasmas](#)


Journal of Vacuum Science & Technology B: Microelectronics and Nanometer Structures Processing, Measurement, and Phenomena **25**, 1640 (2007); <https://doi.org/10.1116/1.2781550>

[Investigation of etching properties of metal nitride/high-*k* gate stacks using inductively coupled plasma](#)

Journal of Vacuum Science & Technology A **23**, 964 (2005); <https://doi.org/10.1116/1.1927536>



HIDEN
ANALYTICAL




Instruments for Advanced Science

- Knowledge,
- Experience,
- Expertise


Click to view our product catalogue

Contact Hiden Analytical for further details:
www.HidenAnalytical.com
info@hideninc.com



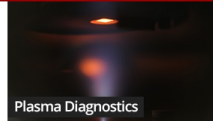
Gas Analysis

- ▶ dynamic measurement of reaction gas streams
- ▶ catalysis and thermal analysis
- ▶ molecular beam studies
- ▶ dissolved species probes
- ▶ fermentation, environmental and ecological studies




Surface Science

- ▶ UHV TPD
- ▶ SIMS
- ▶ end point detection in ion beam etch
- ▶ elemental imaging - surface mapping



Plasma Diagnostics

- ▶ plasma source characterization
- ▶ etch and deposition process reaction kinetic studies
- ▶ analysis of neutral and radical species



Vacuum Analysis

- ▶ partial pressure measurement and control of process gases
- ▶ reactive sputter process control
- ▶ vacuum diagnostics
- ▶ vacuum coating process monitoring



Dry etching of TaN/HfO₂ gate-stack structure in BCl₃/Ar/O₂ inductively coupled plasmas

M. H. Shin, M. S. Park, and N.-E. Lee^{a)}

School of Materials Science and Engineering, Sungkyunkwan University, Suwon, Kyunggi-do 440-746, Korea and Center for Advanced Plasma Surface Technology, Sungkyunkwan University, Suwon, Kyunggi-do 440-746, Korea

Jiyoung Kim

Department of Electrical Engineering, The University of Texas at Dallas, Richardson, Texas 75083

Chung Ywong Kim and Jinho Ahn

School of Materials Science and Engineering, Hanyang University, Seoul 133-791, Korea

(Received 5 May 2005; accepted 15 May 2006; published 22 June 2006)

In this work, etching characteristics of TaN(200 nm)/HfO₂(80 nm) gate-stack structures on Si substrate were investigated by varying the process parameters such as BCl₃/(BCl₃+Ar+O₂) gas mixing ratio (Q), top-electrode power, dc self-bias voltage (V_{dc}), and overetch time in an inductively coupled plasma etcher. To understand the role of the etch gas chemistry, we measure the relative changes in the optical emission intensity of ions and radicals in the plasma as well as in the chemical binding states of the etched TaN surfaces. We used optical emission spectroscopy and x-ray photoelectron spectroscopy respectively. The results showed that BCl₃/Ar/O₂ plasma is more effective in etching the oxidized TaN than Cl₂/Ar/O₂ or HBr/Ar/O₂ plasma. It is believed that the B radical species removes the oxygen atoms on the oxidized TaN surface more effectively by forming volatile boron-oxygen-chlorine compounds, such as trichloroboroxin (BOCl)₃, boron oxychloride (BOCl), and boron dioxide. The measurement data also indicated that high etch selectivities of the TaN to the HfO₂ layer could be obtained at the low V_{dc} , high top-electrode power, and shorter overetch time. © 2006 American Vacuum Society. [DOI: 10.1116/1.2210944]

I. INTRODUCTION

Development of advanced high- k gate dielectrics and their integration into advanced nanoscale complementary-metal-oxide-semiconductor (CMOS) devices below the 50 nm technology node have gained considerable attention recently because of the need to replace ultrathin SiO₂ or nitrided SiO₂ gate dielectrics. To integrate the high- k gate dielectric materials in nanoscale CMOS devices, metal gate electrodes are expected to be used in the future. An important consideration in selecting metal gate electrodes is the work-function value and their processibility for integration. Currently, to integrate the Hf-based high- k dielectric materials, including HfO₂,¹⁻⁴ HfON,^{5,6} HfAlO,⁷ HfSiO,⁸ and HfSiON,^{9,10} the metal gate electrode materials including TaN,^{6,10-13} TiN,^{4,13,14} HfN,^{3,15} WN,¹³ TaSiN,^{2,16} and metal silicides¹³ are being widely studied for next-generation nanoscale CMOS devices.

Adoption of these materials imposes integration problems. Among many integration issues, selective etching of metal gate electrodes and the high- k gate dielectrics over the Si substrate is expected to be one of the critical steps in the process integration of the front end of the line (FEOL).¹⁷ For patterning of the metal gate electrode/high- k structure, two integration schemes can possibly be employed. In the first case, the metal gate electrode is selectively etched with a high etch selectivity against the high- k dielectric layer, and

then the high- k dielectric layer is removed. After the metal gate electrode is etched, the remaining high- k dielectric layer needs to be removed by a wet-etch¹⁸⁻²⁰ and/or dry-etch processes²⁰⁻²⁹ with a high etch selectivity to the Si substrate. In the second method, the metal gate electrode/high- k dielectric stacks can be selectively etched in one step at a time with the same etch chemistry over the Si source/drain regions. In this case, a very high etch selectivity of the gate stacks to the Si substrate is also needed to minimize the Si loss at the ultrashallow source/drain regions. In both methods, the etch selectivity of the etched layers (metal electrode or high- k dielectrics) to the underlayers (high- k dielectrics or Si substrate) is one of the most important parameters in patterning the gate-stack structures.

The previous reports on the etch rate selectivity of the high- k HfO₂ to the Si substrate in the SF₆/Ar and Cl₂/Ar inductively coupled plasma²⁰ (ICP) and ZrO₂ etching in the electron cyclotron resonance (ECR) BCl₂/Cl₂ plasmas^{24,25} showed etch selectivities of less than 1 and 1.5, respectively. These results indicate that a high etch selectivity of the typical high- k dielectric to the Si substrate is difficult to obtain. Therefore, a two-step etching of the metal gate electrode followed by high- k dielectric removal might be a practical solution. For the practical applications during the process integration, therefore, the low etch selectivity of the high- k dielectrics to the Si substrate and difficulty in removing of etch residues after etching,^{18,19} rather than the etch rate itself, are the limiting factors in gate patterning. In this aspect,

^{a)}Author to whom correspondence should be addressed; electronic mail: nelee@skku.edu

etching process development with a high etch selectivity of the metal gate electrode to the high-*k* dielectric is required.

In this report, etch rates and etch selectivity of TaN/HfO₂ gate-stack structures on Si substrate were investigated by varying the process parameters such as BCl₃/(BCl₃+Ar+O₂) gas mixing ratio, top-electrode power, bottom bias-electrode power, and overetch time in an ICP etcher. Optical emission spectroscopy (OES) of the plasma in the chamber and x-ray photoelectron spectroscopy (XPS) of the etched TaN surfaces were also done to understand the etch mechanism of the TaN/HfO₂ stack structure.

II. EXPERIMENT

Etching experiments were carried out in a modified commercial 8 in. ICP etching unit having a 3.5 turn spiral copper coil on the top of chamber separated by a 1-cm-thick quartz window and pumped by a turbo molecular pump backed by a dry/booster pump. The schematic of the system was described elsewhere.^{30,31} Substrate holder temperature during etching was kept constant by circulating cooling water at 18 °C. The samples were fixed on an 8 in. wafer placed on the substrate holder using a heat-conductive paste, DC 340 (Dow Corning). A top-electrode power of 13.56 MHz was applied to the top coil electrode to induce ICP. Another 13.56 MHz of bottom-electrode power was applied to the substrate holder to induce dc self-bias voltage (V_{dc}) to the wafer.

For sample preparation, the HfO₂ layer with a thickness of 80 nm was deposited on the Si(001) substrate by rf reactive sputtering of the Hf target using O₂/Ar sputtering gas. Here, a relatively thick HfO₂ layer was used to evaluate the etch selectivity. The 200-nm-thick TaN layer was deposited on the HfO₂/Si(001) substrate by dc magnetron sputtering of the TaN target using Ar sputtering gas. Etching masks for the TaN/HfO₂/Si(001) samples were patterned using an optical lithography of positive photoresist (PR) with a thickness of ~1.8 μm.

First, TaN etch rates were measured by partially etching the TaN layers in the TaN/HfO₂ stack with the photoresist mask. Then, the TaN/HfO₂ stack structures were etched so that the samples were partially etched down to the HfO₂ layer. Etch depths of the TaN and HfO₂ films were obtained by a field emission scanning electron microscopy (FE-SEM). The overetch time was 30 s, except for the experiment on the effect of overetch time on etch selectivity (see Fig. 7). Using the premeasured TaN and HfO₂ etch rates, TaN/HfO₂ etch selectivity was estimated.

To understand the etching mechanism of TaN and HfO₂, OES was used to investigate the species in the plasma. Emission spectra at the wavelength range of 200–1000 nm were detected in this experiment. Species with optical emission were monitored as the peak intensities of characteristic optical lines. The optical emission lines corresponding to Ar, B, and Cl ions or radicals were mainly monitored in the work. The surface binding states of the TaN thin film etched in the BCl₃/Ar/O₂ plasmas were investigated using XPS. The Mg Kα source for XPS provides nonmonochromatic x rays

at 1253.6 eV. XPS narrow-scan spectra of all the interesting regions were recorded with a pass energy of 20 eV. The takeoff angle, which is an angle between the axis of the detector and the substrate, was kept at 90° and the x ray was incident on the substrate surface with the angle of 54.7°. The binding energy of 244.6 eV corresponding to the C 1s spectra was used as a reference peak position.

III. RESULTS AND DISCUSSIONS

A. Effect of TaN surface oxidation

In this experiment, we found that etching of TaN layers depended greatly on the surface condition of the TaN layers. To elucidate the effects of the TaN surface condition on TaN etching, we carried out the chemical and structural analyses of the TaN surfaces before etching using the various etch chemistries based on Cl₂, BCl₃, and HBr gases. The deposited TaN layers were exposed to the air before etching. Etching experiments were performed by using the Cl₂(BCl₃,HBr)/Ar/O₂ chemistries. The results showed that the TaN samples used in this experiment could not be etched in the Cl₂/Ar/O₂ and HBr/Ar/O₂ plasmas, but could be etched in the BCl₃/Ar/O₂ plasma.

To find the reason for the difficulty in etching the surface-oxidized TaN, chemical and microstructural analyses of the deposited TaN layers were performed. Figures 1(a) and 1(b) show the FE-SEM and cross-sectional transmission electron microscopy (XTEM) micrographs of the unetched TaN layers, and Fig. 1(c) shows the XPS spectra of the unetched TaN surfaces. The FE-SEM and XTEM images in Figs. 1(a) and 1(b), respectively, show the formation of the very thin oxidized layer with a thickness of ~5 nm. XPS spectra in Fig. 1(c) also show the strong Ta–O peaks due to the surface oxidation of the TaN layer. Energy dispersion spectroscopy (EDS) mapping in the XTEM also confirmed the oxidation of the TaN surface. In the case of the TaO_xN_y layer forming on the TaN surface, the chemical reaction of Cl radicals with the oxygen on the TaO_xN_y surface is required. Because the chemical reaction of Cl with Ta atoms leading to the breakup of Ta–O bonds requires high energy, the etching reaction can be limited because of the surface oxidation of the TaN layers. The previous etching experiments of TaN by our group indicated that well-controlled reactive-sputtered TaN could be etched in the Cl₂/Ar (Ref. 30) and Cl₂/Ar/SF₆ (Ref. 30) ICP. Other TaN etching experiments, however, showed the difficulty in plasma etching of the oxidized TaN layers.²⁹ The differences in the present experiments compared to the previous experiments^{30,31} are presumably attributed to the longer air exposure time and the deposition method. Because the TaN layers can be etched well using BCl₃/Ar/O₂ regardless of the TaN surface conditions, we investigated plasma etching characteristics of the TaN/HfO₂ stack structure in the BCl₃/Ar/O₂ inductively coupled plasmas by varying the various process conditions.

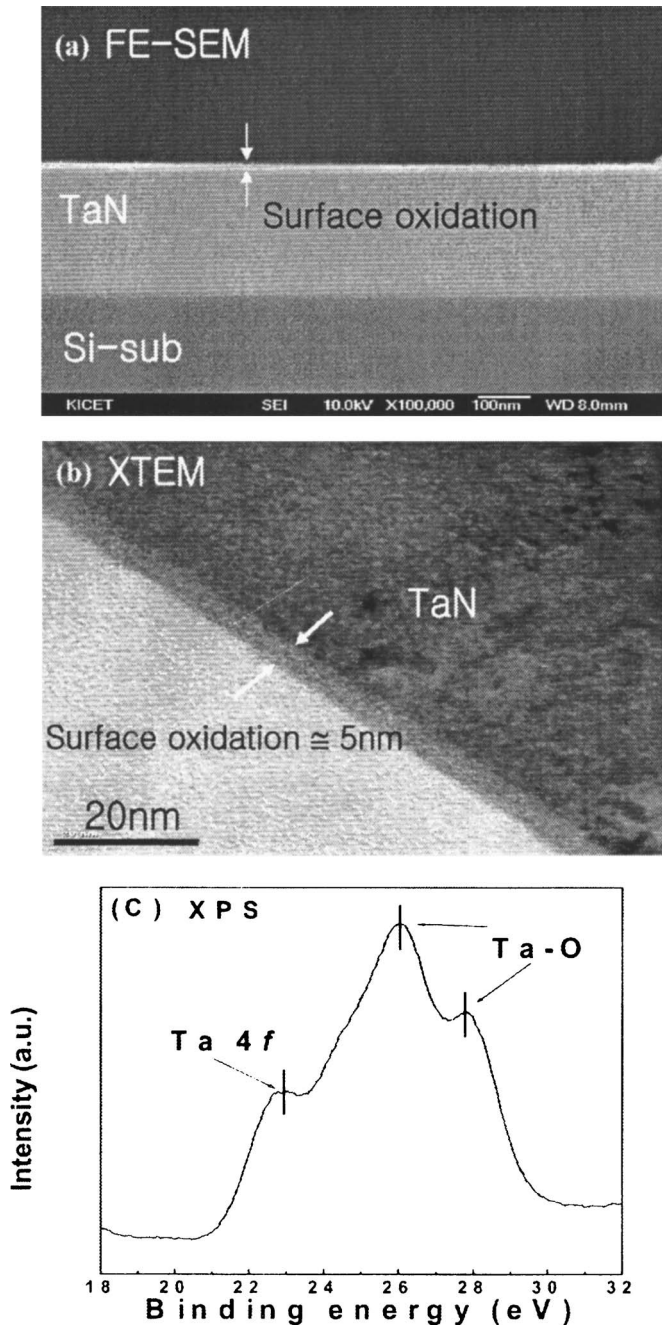


FIG. 1. (a) FE-SEM and (b) XTEM micrographs of the unetched TaN, and (c) XPS spectra obtained from the unetched TaN layer.

B. Effect of $\text{BCl}_3/(\text{BCl}_3+\text{Ar}+\text{O}_2)$ gas mixing ratio Q

First, etching characteristics of the TaN/HfO₂ gate structures were measured in the $\text{BCl}_3/\text{Ar}/\text{O}_2$ ICP by varying the $\text{BCl}_3/(\text{BCl}_3+\text{Ar}+\text{O}_2)$ gas flow ratio Q from 0 to 1 at a fixed O_2 flow of 5 SCCM (SCCM denotes cubic centimeter per minute at STP) and a total flow rate of 55 SCCM. The top-electrode power and V_{dc} were fixed at 300 W and -100 V, respectively. TaN etch rate and etch selectivity of the TaN to the PR and HfO₂ layer in the PR/TaN/HfO₂ gate structure were measured, and the results are shown in Fig. 2. As Q increased from 0 to 0.2, the TaN etch rate increased rapidly

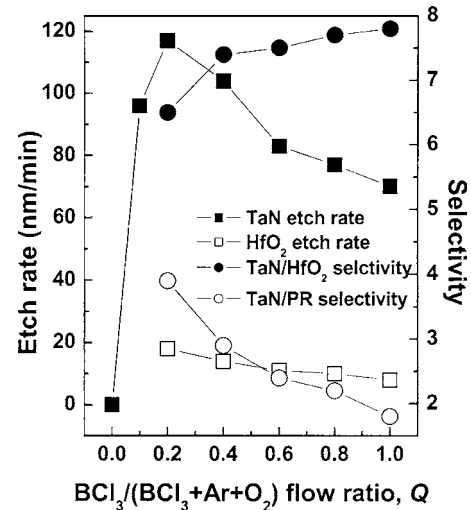


FIG. 2. Etch rates of TaN and HfO₂ and etch selectivity of the TaN layer to the PR and the HfO₂ layer as a function of the $\text{BCl}_3/(\text{BCl}_3+\text{Ar}+\text{O}_2)$ gas mixing ratio Q .

and then gradually decreased at $Q \geq 0.3$. On the other hand, the HfO₂ etch rate slowly increased as Q increased. Figure 2 also shows the etch selectivities of TaN to PR and HfO₂ with varying Q . As Q increased from 0.2 to 1, the etch selectivity of TaN to-PR decreased from ~ 3.9 to ~ 1.8 and that of TaN to HfO₂ increased from ~ 6.5 to ~ 8.8 .

To find a correlation between the etch rates of the TaN and HfO₂ layers and any change in the density of the species in the plasmas, we measured the optical emission spectra of the $\text{BCl}_3/\text{Ar}/\text{O}_2$ inductively coupled plasmas as a function of Q . The optical emission spectra of the Cl^+ ions (268.8 and 544.4 nm), B radicals (608.0 nm), Ar^+ ions (738.0 nm), and Ar (763.5 and 811.5 nm) were monitored, and their intensities are shown in Fig. 3. The optical emission intensities of

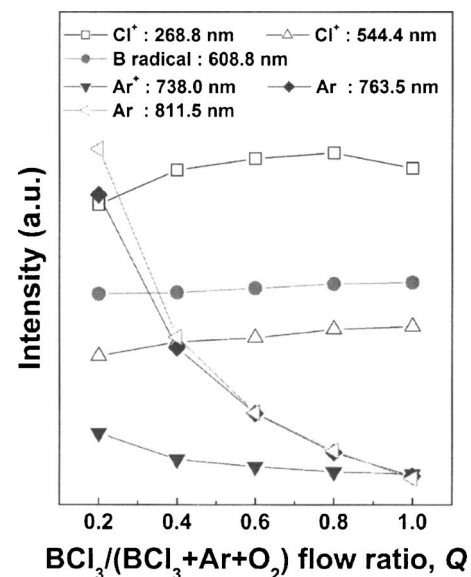


FIG. 3. Optical emission intensity of Cl ions, B radicals, Ar ions, and Ar radicals by OES as a function of Q at a fixed O_2 flow rate of 5 SCCM.

the B radicals and Cl⁺ ions only slightly increased at the range of Q from 0.2 to 1, and those of the Ar atoms and Ar⁺ ions gradually decreased as Q increased. Emission signal intensity corresponding to the Cl radicals was too small to observe from the OES spectra due to the limited detection sensitivity in the our experimental setup, but the Cl radical emission intensity would be similar to the trend of Cl⁺ ions with the BCl₃ flow increase. A significant observation is that the optical emission intensity of the Cl ions and B radicals is not correlated with the trend in the TaN etch rate in Fig. 2.

Because halide etch by-products of TaCl₅ and TaF₅ have relatively low volatility due to the relatively high boiling points of 242 (Ref. 32) and 230 °C,³³ respectively, an ion-assisted etching mechanism is needed for the Ta-containing materials.^{32,34–38} The etch rates of TaN are expected to strongly follow the behavior of the neutral-to-ion flux ratio Γ_N/Γ_I provided that the reaction of Cl radicals with TaN, i.e., the chlorination, is a dominant factor in determining TaN etch rates.^{40,41} In fact, the correlation between the etch rate and Cl⁺ emission intensity from Figs. 2 and 3 suggests that the etch reaction of TaN films is affected by a chemical reaction with Cl-containing species, with TaN leading to the formation of TaCl_{*x*}, whose removal is assisted by ion bombardment.^{41,42} For a large Γ_N/Γ_I region where the Ar flow is small, i.e., Q is large, the reaction becomes ion-flux limited and as a result the etch rate is governed by the ion-enhanced removal of the etch by-products on the surface. Therefore, the TaN etch rate is expected to decrease as the Ar flow decreases, as seen in Fig. 2. For a small Γ_N/Γ_I region where the Ar flow is large, i.e., Q is small, the etch reaction becomes chemical-reaction limited and the etch rate is determined by the reaction rate of reactive Cl and B radicals with the TaN layers. In this situation, the etch rate is expected to increase due to the increasing radical density with the Q to be increased, as seen in Fig. 2.

XPS measurements were made on the TaN surfaces etched without the PR mask to examine the chemical binding states and residues on the etched surface. The Ta 4*f*, O 1*s*, and N 1*s* spectra for various Q values are shown in Figs. 4(a)–4(c), respectively. The peak positions are referenced to the binding energy of 244.6 eV corresponding to the C 1*s* spectra. The B 1*s* and Cl 2*p* spectra for various Q values were also obtained but not included here because the B 1*s* and Cl 2*p* intensities were at the background level and not changed with the Q increase. The negligible XPS signal from the B and Cl surface elements indicates the presence of a negligibly small amount of Ta chloride (TaCl_{*x*}) or TaO_{*x*}Cl_{*y*} residue due to an effective removal of the etch by-products. The observed intensity in the C 1*s* spectra (not shown here) was presumably attributed to surface contamination due to the use of photoresist for etching. In Fig. 4(a), the Ta 4*f*_{5/2} and Ta 4*f*_{7/2} peaks were observed at the binding energies of 24.0 and 22.1 eV, respectively.⁴³ The Ta 4*f* XPS spectra in Fig. 4(a) show that unetched and etched TaN surfaces are strongly oxidized. The intensity of the Ta–O peaks from the etched TaN was lower than that from the as-deposited film, presumably due to the reaction of the O with the B radicals

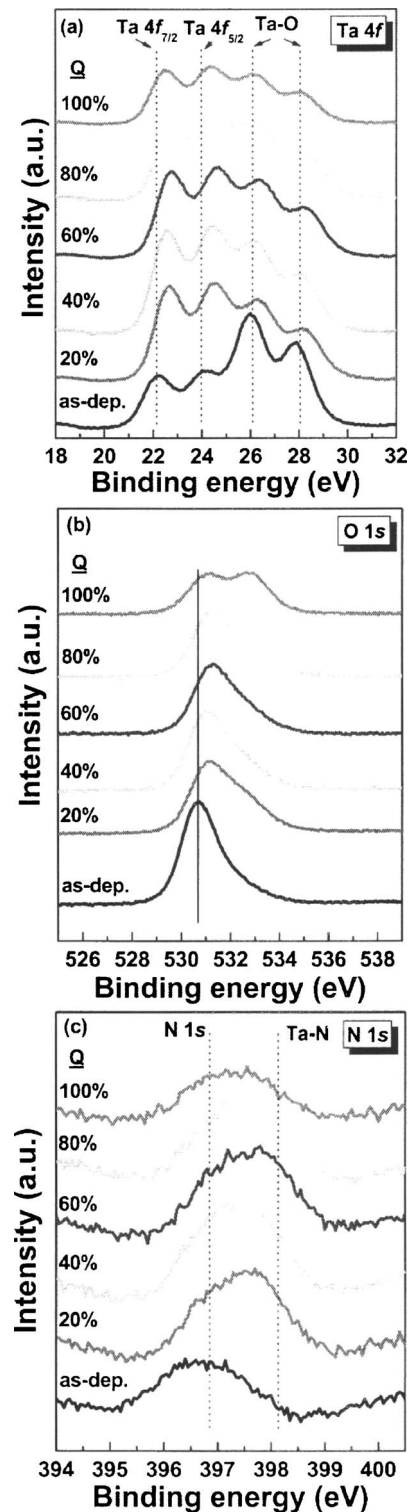


Fig. 4. XPS spectra obtained from the etched blanket TaN(200 nm)/Si(001) substrate; (a) Ta 4*f*, (b) O 1*s*, and (c) N 1*s*. The samples were etched by varying the flow ratio Q at a fixed O₂ flow rate of 5 SCCM.

leading to the reduction in oxygen concentration. The O 1*s* spectra obtained from the as-deposited and etched samples are shown in Fig. 4(b). The O 1*s* peak corresponding to the Ta–O bonding was observed at a binding energy of 530.7 eV.^{44,45} The higher binding-energy peak located at

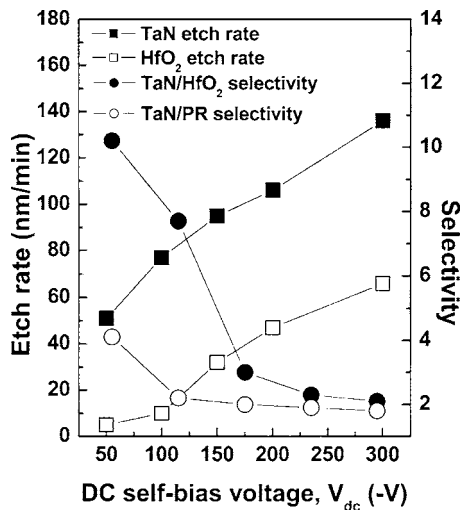


FIG. 5. Etch rates of TaN and HfO₂ and etch selectivity of the TaN layer to the PR and the HfO₂ layer as a function of the dc self-bias voltage V_{dc} .

532.7 eV, observed for the case of $Q=100\%$, is usually attributed to surface contamination.⁴⁶ For the etched sample, the O 1s peaks are shifted toward higher energies in the range of 531.2–531.3 eV, representing a shift of 0.5–0.6 eV. The N 1s spectra in Fig. 4(c) show that the position of the peaks was shifted toward the higher binding energy, probably due to the reaction of Cl radicals with the TaN surface.

The XPS measurement data suggest that the BCl₃/Ar/O₂ plasma is effective in etching the oxidized TaN layers. It is believed that the B radical species removes the oxygen in the oxidized TaN surface by forming volatile boron-oxygen-chlorine compounds, such as trichloroboroxin (BOCl)₃, boron oxychloride (BOCl), and boron dioxide (BO₂).^{47,48} In particular, (BOCl)₃ is a stable gas with a large negative heat of formation formed by an exothermic reaction of $6\text{BCl}_3 + 3\text{O}_2 \rightarrow 2(\text{BOCl})_3 + 6\text{Cl}$.⁴⁹ In addition, Cl radical species generated from BCl₃ gas can remove the Ta atoms in TaN by forming volatile TaCl_x through an ion-enhanced chemical etching process. Similar enhanced etching of other metal oxides in the BCl₃-containing plasmas has also been observed.^{50,51}

C. Effect of bottom-electrode power

To investigate the effect of V_{dc} on the etch rates and etch selectivity in the BCl₃/Ar/O₂ plasma, etching experiments were carried out by varying V_{dc} , while keeping the total gas flow at 55 SCCM and the fixed O₂ flow at 5 SCCM. The Q was fixed at 80% and the top ICP electrode power was fixed at 300 W.

The etch rate and etch selectivity results are shown in Fig. 5. The etch rates were monotonically increased from ~51–~136 and ~5–~66 nm/min for TaN and HfO₂, respectively, while varying the V_{dc} from –50 to –300 V. The etch selectivities of TaN to PR and HfO₂ decreased due to an increase of V_{dc} . The maximum selectivities for TaN to PR and HfO₂ in this experiment were ~4.1 and ~10.2.

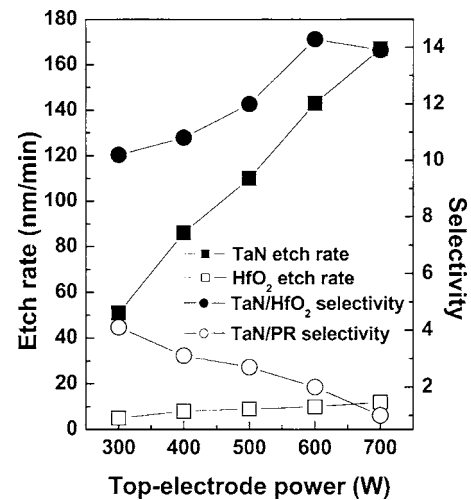


FIG. 6. Etch rates of the TaN and HfO₂ layers and etch selectivity of TaN layer to the PR and HfO₂ layer as a function of the ICP electrode power.

The increased etching rate with the V_{dc} increase is associated with the enhanced sputtering on the TaN and HfO₂ surfaces by an increase of ion-bombardment energy leading to enhanced removal of etch by-products. In this ion-limited process regime (see Fig. 3), ion-bombardment energy absorbed by the surface accelerates the etching reaction step.⁵² However, because the etch rate of the HfO₂ increased more rapidly compared to that of the TaN because of the more physical etching characteristics of the layers, TaN/HfO₂ etch selectivity decreased. Under the experimental conditions here, the etch selectivities decreased as the physical component of the etch mechanism became more prominent.

D. Effect of top-electrode power

The etch rates and etch selectivities obtained as a function of the top ICP electrode power at V_{dc} of –50 V and Q of 80% are shown in Fig. 6. Etching was performed by varying the ICP electrode power range of 300–700 W. As shown in Fig. 6, the etch rates were monotonically increased from ~51–~167 and ~5–~12 nm/min for the TaN and HfO₂ layers, respectively, while varying the ICP electrode power from 300 to 700 W. The selectivity of the TaN to the PR was decreased with the ICP electrode power increase because the chemical component of the etch mechanism became more prominent. However, the selectivity of the TaN to the HfO₂ layers gradually increased and then slightly decreased at the top-electrode power of ≥ 600 W. The maximum etch selectivities of TaN to PR and HfO₂ were ~4.1 and ~14.3, respectively.

The etch rate of TaN increased monotonically as the ICP electrode power increased, indicating that only one mechanism is operative for all the experimental conditions. The reaction regime at $Q=0.8$ in Fig. 2 belongs to the ion-flux-limited regime with the large Γ_N/Γ_I . As discussed already, etch rate is affected by the density of reactive ions and ion energy flux in the plasma, and etch rate is usually enhanced by an increased rate of chemical reactions in etched

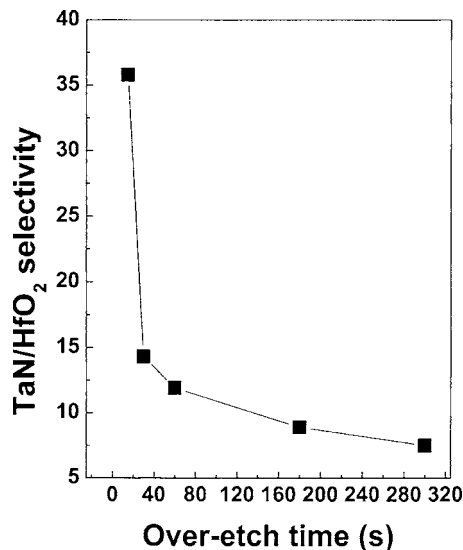


FIG. 7. Etch selectivity of TaN layer to the HfO₂ layer as a function of the overetch time.

surfaces.^{52,53} In the present experiments, the increases in the ICP electrode power and hence the increase in the density of the ion species are believed to be responsible for the monotonic increase in the etch rate of TaN. But the HfO₂ etch rate varied very little despite of the increased plasma density caused by the higher ICP electrode power. The HfO₂ etch rate also increased, but more slowly as the top-electrode power increased. As a result, the etch selectivity remained at a high value due to the low HfO₂ etch rates.

E. Effect of overetch time on etch selectivity

To investigate the effect of overetch time of the HfO₂ underlayer on the etch selectivities of the TaN to the HfO₂ layer, etch experiments were carried out by varying the overetch time, while keeping the total gas flow at 55 SCCM, the fixed O₂ flow at 5 SCCM, the Q at 80%, the top-electrode power at 600 W, and the V_{dc} at -50 V. The etch selectivity results are shown in Fig. 7. The TaN/HfO₂ etch selectivity increases due to a decrease of the overetch time. Etch selectivities increased from ~ 7.5 to ~ 35.8 as the overetch times were decreased from 300 to 15 s.

Lemme *et al.*⁵⁴ reported that through several steps and tradeoffs under certain process conditions during poly-Si etching, a complete etch stop is possible on SiO₂ for a limited amount of time. Even after this etch stop-time expires, a selectivity of over 200:1 (polysilicon:SiO₂) has been achieved. This indicates that etch selectivity is strongly affected by the initiation time for etching. Extremely high selectivity is only achieved if the overetch time is shorter than the initiation time. In the present experiments, the shorter overetch time increases the TaN/HfO₂ selectivity, probably because the overetch time approaches the initiation time.

IV. CONCLUSION

The etching characteristics of TaN(200 nm)/HfO₂(100 nm) gate-stack structures on the Si substrate were investigated in BCl₃/Ar/O₂ inductively coupled plasmas by varying the process parameters such as the etch gas mixing ratio (Q), dc self-bias voltage (V_{dc}), top-electrode power, and overetch time.

We found that the surface oxidation of the TaN layers significantly affected the etching characteristics of the TaN layers. Surface-oxidized TaN layers could not be etched in the Cl₂/Ar/O₂ and HBr/Ar/O₂ plasmas, but could be etched in the BCl₃/Ar/O₂ plasma. Enhanced etching in the BCl₃/Ar/O₂ plasma is presumably attributed to the efficient breaking of Ta–O bonds due to the reaction of B radicals with the oxygen on the etched surface, leading to the formation of volatile B-containing etch by-products.

The etch rates of TaN and HfO₂ layers under varied Q were found to be determined by an interplay between the chemical reaction of reactive B and Cl radicals and an ion-enhanced removal process of the reaction by-products. For a maximum etch rate, an optimum gas mixing ratio Q of BCl₃/(BCl₃+Ar+O₂) is required.

The enhanced TaN/HfO₂ etch selectivity could be obtained at the reduced V_{dc} and higher top-electrode power because the etching rate of HfO₂ layer is governed by stronger ion-enhanced sputtering compared to the TaN etching. Also, the overetch time of the HfO₂ layers is a strong parameter in determining the TaN/HfO₂ etch selectivity. Enhanced etch selectivity at the shorter overetch time is presumably related to the initiation time for the onset of the etching reaction.

ACKNOWLEDGMENTS

This work was supported through the System IC 2010 program by the Ministry of Commerce, Industry, and Energy, the Ministry of Science and Technology, and in part through the Center of Excellency program of the Korea Science and Engineering Foundation (Grant No. R-11-2000-086-0000-0).

- ¹S. J. Lee, C. H. Choi, A. Kamath, R. Clark, and D. L. Kwong, *IEEE Electron Device Lett.* **24**, 105 (2003).
- ²A. Vandooren *et al.*, *IEEE Electron Device Lett.* **24**, 342 (2003).
- ³C. Ren *et al.*, *IEEE Electron Device Lett.* **25**, 580 (2004).
- ⁴A. Vandooren *et al.*, *IEEE Trans. Nanotechnol.* **2**, 324 (2003).
- ⁵C. H. Choi, T. S. Jeon, R. Clark, and D.-L. Kwong, *IEEE Electron Device Lett.* **24**, 215 (2003).
- ⁶C. S. Kang *et al.*, *IEEE Trans. Electron Devices* **51**, 220 (2004).
- ⁷S. H. Bae, C. H. Lee, R. Clark, and D. L. Kwong, *IEEE Electron Device Lett.* **24**, 556 (2003).
- ⁸T. Iwamoto *et al.*, *Tech. Dig. - Int. Electron Devices Meet.* **2003**, 27.5.1.
- ⁹A. L. P. Rotondaro, M. R. Visokay, V. A. Shanware, J. J. Chambers, and L. Colombo, *IEEE Electron Device Lett.* **23**, 603 (2002).
- ¹⁰X. Wang, J. Liu, F. Zhu, N. Yamada, and D. L. Kwong, *IEEE Trans. Electron Devices* **51**, 1798 (2004).
- ¹¹R. E. Nieh *et al.*, *IEEE Trans. Electron Devices* **50**, 333 (2003).
- ¹²K.-J. Choi and S. G. Yoon, *Electrochem. Solid-State Lett.* **7**, G47 (2004).
- ¹³J. K. Schaeffer *et al.*, *J. Vac. Sci. Technol. B* **21**, 11 (2003).
- ¹⁴J. Westlinder, T. Schram, L. Pantisano, E. Cartier, A. Kerber, G. S. Lujan, J. Olsson, and G. Groeseneken, *IEEE Electron Device Lett.* **24**, 550 (2003).
- ¹⁵H. Yu, M.-F. Li, and D.-L. Kwong, *IEEE Trans. Electron Devices* **51**, 609

- (2004).
- ¹⁶P. Alen, T. Aaltonen, M. Ritala, M. Leskela, T. Sajavaara, J. Keinonen, J. C. Hooker, and J. W. Maes, *J. Electrochem. Soc.* **151**, G523 (2004).
- ¹⁷I. De, D. Johri, A. Srivastava, and C. M. Osburn, *Solid-State Electron.* **44**, 1077 (2000).
- ¹⁸M. A. Quevedo-Lopez, M. El-Bouanani, R. M. Wallace, and B. E. Gnade, *J. Vac. Sci. Technol. A* **20**, 1981 (2002).
- ¹⁹J. Chen, W. J. Yoo, D. S. H. Chan, and D.-L. Kwong, *Electrochem. Solid-State Lett.* **7**, F18 (2004).
- ²⁰S. Norasesthetkul *et al.*, *Appl. Surf. Sci.* **187**, 75 (2002).
- ²¹J. A. Britten, H. T. Nguyen, S. F. Falabella, B. W. Shore, M. D. Perry, and D. H. Raguin, *J. Vac. Sci. Technol. A* **14**, 2973 (1996).
- ²²K. Pelhos *et al.*, *J. Vac. Sci. Technol. A* **19**, 1361 (2001).
- ²³L. Sha, B. O. Cho, and J. P. Chang, *J. Vac. Sci. Technol. A* **20**, 1525 (2002).
- ²⁴L. Sha, R. Puthenkovilakam, Y. S. Lin, and J. P. Chang, *J. Vac. Sci. Technol. B* **21**, 2420 (2003).
- ²⁵L. Sha and J. P. Chang, *J. Vac. Sci. Technol. A* **21**, 1915 (2003).
- ²⁶L. Sha and J. P. Chang, *J. Vac. Sci. Technol. A* **22**, 88 (2004).
- ²⁷J. Chen, K. M. Tan, N. Wu, W. J. Yoo, and D. S. H. Chan, *J. Vac. Sci. Technol. A* **21**, 1210 (2003).
- ²⁸S. G. Woo, S. H. Kim, S. Y. Ju, J. H. Son, and J. H. Ahn, *Jpn. J. Appl. Phys., Part 1* **39**, 6996 (2000).
- ²⁹J. Chen, W. J. Yoo, Z. Y. L. Tan, Y. Wang, and D. S. H. Chan, *J. Vac. Sci. Technol. A* **22**, 1552 (2004).
- ³⁰M. H. Shin, S. W. Na, N.-E. Lee, and J. H. Ahn, *Thin Solid Films* (in press).
- ³¹M. H. Shin, S. W. Na, N.-E. Lee, T. K. Oh, J. Y. Kim, T. H. Lee, and J. H. Ahn, *Jpn. J. Appl. Phys., Part 1* **44**, 5811 (2005).
- ³²S. G. Woo, S. H. Kim, S. Y. Ju, J. H. Son, and J. Ahn, *Jpn. J. Appl. Phys., Part 1* **39**, 6996 (2000).
- ³³A. J. van Roosmalen, J. A. G. Baggerman, and S. J. H. Brader, *Dry Etching for VLSI* (Plenum, New York, 1991), p. 121.
- ³⁴Y. Iba, F. Kumasaka, H. Aoyama, T. Taguchi, and M. Yamabe, *Jpn. J. Appl. Phys., Part 2* **37**, L824 (1998).
- ³⁵T. Tsuchizawa, C. Takahashi, M. Shimada, S. Uchiyama, T. Ono, and M. Oda, *Microelectron. Eng.* **53**, 595 (2000).
- ³⁶T. Tsuchizawa, H. Iriguchi, C. U. Takahashi, M. Shimada, S. Uchiyama, and M. Oda, *Jpn. J. Appl. Phys., Part 1* **39**, 6914 (2000).
- ³⁷K. P. Lee, K. B. Jung, R. K. Singh, S. J. Pearton, C. Hobbs, and P. Tobin, *J. Electrochem. Soc.* **146**, 3794 (1999).
- ³⁸H. Shimada and K. Maruyama, *Jpn. J. Appl. Phys., Part 1* **43**, 1768 (2004).
- ³⁹N. C. M. Fuller, I. P. Herman, and V. M. Donnelly, *J. Appl. Phys.* **90**, 3182 (2001).
- ⁴⁰A. M. Efremov, D. P. Kim, and C. I. Kim, *Thin Solid Films* **435**, 232 (2003).
- ⁴¹Y. C. Kim and C. I. Kim, *J. Vac. Sci. Technol. A* **19**, 2676 (2001).
- ⁴²K. H. Kwon, C. I. Kim, S. J. Yun, and G. Y. Yeom, *J. Vac. Sci. Technol. A* **16**, 2772 (1998).
- ⁴³A. M. Lemonds, J. M. White, and J. G. Ekerdt, *Surf. Sci.* **527**, 124 (2003).
- ⁴⁴E. Atanassova, T. Dimitrova, and J. Koprinarova, *Appl. Surf. Sci.* **84**, 193 (1995).
- ⁴⁵A. Muto, F. Yano, Y. Sugawara, and S. Lijima, *Jpn. J. Appl. Phys., Part 1* **33**, 2699 (1994).
- ⁴⁶L. Chen and R. W. Hoffman, *J. Vac. Sci. Technol. A* **11**, 2303 (1993).
- ⁴⁷D. W. Hess, *Solid State Technol.* **1981**, 189.
- ⁴⁸K. Tokunaga, F. C. Redeker, D. A. Danner, and D. W. Hess, *J. Electrochem. Soc.* **128**, 851 (1981).
- ⁴⁹J. Blauer and M. Farber, *J. Chem. Phys.* **39**, 158 (1963).
- ⁵⁰K. Pelhos *et al.*, *J. Vac. Sci. Technol. A* **19**, 1361 (2001).
- ⁵¹T.-H. An, J.-Y. Park, G.-Y. Yeom, E.-G. Chang, and C.-I. Kim, *J. Vac. Sci. Technol. A* **18**, 1373 (2000).
- ⁵²J. Ding, J.-S. Jenq, G.-H. Kim, H. L. Maynard, J. S. Hamers, N. Hershkoviz, and J. W. Taylor, *J. Vac. Sci. Technol. A* **11**, 1283 (1993).
- ⁵³F. A. Khan and I. Adesida, *Appl. Phys. Lett.* **75**, 2268 (1999).
- ⁵⁴M. C. Lemme, T. Mollenhauer, H. Gottlob, W. Henschel, J. Efavi, C. Welch, and H. Kurz, *Microelectron. Eng.* **73**, 346 (2004).